

# Computational Modeling of Nanoparticle Targeted Drug Delivery

Pasupuleti Anusha<sup>1</sup>, Dr. V. Venkata Ramana<sup>2</sup>, Dr. MV Rathnamma<sup>3</sup>

<sup>1</sup>*BTech 3rd Year, Metallurgical and Materials Engineering National Institute of Technology  
Surathkal, Karnataka anushap.211mt035@nitk.edu.in*

<sup>2</sup>*Professor, Department of CSE KSRM College of Engineering (A), Kadapa - AP  
vvr@ksrmce.ac.in*

<sup>3</sup>*Professor and Principal, Department of CSE KLM College of Engineering, for Women  
Kadapa - AP mvrathnamma@gmail.com*

By using nanotechnology for tailored medication delivery, nanomedicine has great promise as a medical application. Nevertheless, the intricate in vivo circulatory system and the microscopic size of nanoparticles make it very difficult to characterise the targeted distribution process of nanoparticles in a vascular environment. A number of computer models have been created to shed light on the targeted delivery process of nanoparticles and to assist in the design of nanoparticles for optimum delivery in order to make sense of such a complex system. In order to facilitate effective targeted distribution, this article goes over several computational techniques for mDodeleilvttehreednabnyolpnagrticnletadteol:ivery and nanoparticle design. From molecular level ligand-reaction dynamics to continuum vascular flow and particle Brownian adhesion dynamics, the modelling approach sUpsaenr covers it all. It is believed that computer simulation can optimise drug carrier design and forecast the vascular environment particular to each patient.[4]

**Keywords:** Nanomedicine, Nanoparticle, Cancer, Drug Delivery, Computational Modeling..

## 1. Introduction

In general, structures having a size between 1 and 100 nm in at least one dimension are the focus of nanotechnology, which is the study of matter on the nanoscale.<sup>1</sup> There is a wide variety of uses for nanotechnology; "nanomedicine" describes the field's use in the medical field. The potential for medication delivery systems based on nanomedicine to enhance human health in the future of medicine is enormous. Out of all the subfields within nanomedicine, drug delivery accounts for more than 70% of the scholarly articles.<sup>2</sup> Drug delivery[1][2] systems work to enhance patient care

by facilitating the distribution of complex new medications, increasing the bioavailability of current treatments, and allowing for the spatial and temporal tailoring of drugs to significantly decrease adverse effects and maximise efficacy. Realising these game-changing benefits would allow for more individualised prescriptions, easier administration, more patient compliance, fewer dose frequency, and less discomfort for both patients and doctors[3][4]. The use of nanoparticulate systems in diagnostic imaging and tailored therapeutics has grown exponentially within the last decade.three to ten There are many different types of nanoplatforms that have been produced. Some examples include liposomes, polymeric micelles, quantum dots, dendrimers, and Au/Si/polymer shells. Nanomedicine faces several obstacles, despite new evidence of much increased effectiveness of in vivo nanoparticle (NP)[5][6] medication delivery compared to conventional drug delivery methods. Researching medication delivery systems, for instance, is not a simple task that needs further thought and thorough examination[7]. This particular medication methods for capturing the mobility of nanoparticles, including molecular dynamics, Brownian motion, and stochastic approaches like Monte Carlo simulation. Two groups that modelled the transport of spherical NPs to tumours are Shipley et al.<sup>27</sup> and Modok et al.<sup>28</sup>. This article presents a drug delivery model based on the work of Mahmoudi et al. (29), Li et al. (30), and provides several instances of targeted drug administration in vascular settings as well as the fundamental governing equations. Secondly, the approach of coupled Brownian adhesion dynamics is used to characterise particle modelling, where the binding and mobility are Ingenta supplied it such that: analysed Gmauge-st by computational fluid dynamics Negatively affecting vascular flow are individual nanoparticles (NPs) in the bloodstream. Liu et al. (31), Zhang et al. (32), and others modelled. Finally, nuclear particle (NP) deposition in lung air has been the subject of future computer modelling studies[8].We quickly go over the topic of F2i9guArepr2 201e2lin0g1:o3f9ta:0rg9eted medication delivery. presents a framework for multiscale simulation that targets medication administration, spanning from a personalised approach to a continuum model. Recent developments in computer science have made computational modelling an attractive option for the application of targeted medication delivery. Medicated nanoparticles with ligands attached travel through the bloodstream and cling to damaged cells by targeted adhesion. But when hydrodynamic force, adhesion force, and Brownian force all act at once, this process gets intricate. The interaction between ligands and receptors is an especially complex chemical mechanism. When it comes to targeted drug delivery, the efficiency is determined by the surface characteristic of functionalized nanoparticles, which provide focused selectivity. The dynamic delivery mechanism may be better understood with the use of a computational modelling tool, which will allow for more precise nanoparticle design. In this piece, we look at a multiscale computational strategy for tailored medication distribution. To begin with, linear

## **2. Continuum Approach: Drug Dissolution To Convection-Diffusion-Reaction Model Of Drug Delivery**

### **2.1 Introduction**

An essential part of the targeted drug delivery area is the in vivo release, transportation, and

targeted binding of drugs. It is necessary to inject the drug-loaded carriers into the circulatory system before they can travel through, across, and inside tissues, cells, and vessels in order to target the illness location. The targeted disease area is reached when drug-loaded particles, coated with ligands, bind specifically to receptors expressed on the membrane of disease cells. After then, the process is followed by the uptake of drugs by cells and their subsequent release. The three steps of drug delivery—drug dissolution, transport, and binding—can be characterised by the mass conservation law and chemical kinetic reactions, according to the continuum perspective. It is now possible to anticipate the spatial and temporal variation of drug transport in live tissues by combining state-of-the-art computational fluid dynamics (CFD) modelling with in vitro drug release profiles from controlled release platforms. To illustrate the release of drugs into brain tissue, Saltzman and Radomsky<sup>33</sup>[9] created a diffusion kinetics model. The blood-brain barrier, a phenomenon characterised by the selective permeability of blood capillaries, led to the assumption that diffusion primarily dominated the transport mechanism. Data from experiments on the spatial dispersion of drugs supports the prediction made by this simple model. A model in three dimensions (3D) of The study conducted by Wang et al.<sup>34</sup> included a primitive neuroectodermal tumour in a human brain. The computational fluid dynamics (CFD) techniques are used to solve the drug concentration, momentum, and continuity equations all at once throughout the simulation. The role of convective transport of macro- and micromolecular pharmacological agents in the tumor's immediate proximity was investigated using their model. Here we outline the continuous drug delivery model's governing equations and provide several examples to illustrate its use[10][11]

## 2.2. Dissolution of Drug Particles

In order to explain how drugs dissolve and unleash their effects, many mathematical models have been developed and put into use.positions 35–38 Assuming a slow drug-releasing mechanism, the most basic kind of drug dissolution profile is zero-order kinetics.

$$Q - Q_0 = Kt \quad (1)$$

Higuchi<sup>38</sup> formulated following relation to model low soluble drug release problem:

$$f_t = \frac{D(2C - C_s)C_s t}{l} \quad (5)$$

Where C is the drug initial concentration, C<sub>s</sub> is the drug solubility in the matrix media and D is the diffusion coefficient of the drug molecules in the matrix substance.

A few other models are summarized in a review paper by Paulo Casta et al.<sup>41</sup> The commonly used mathematical models are listed in Table I.

## 2.3 Convection-Diffusion-Reaction Model of DrugDelivery

The concentration of nanoparticle c inside a vascular sys- tem can be described by the convection-diffusion equation: constant. Dividing the above equation by Q<sub>0</sub> simplifying

it to:

$$f_0 = kt \quad (2)$$

= – Where  $f_t = 1 - Q_t/Q_0$  is often referred as fraction of drug.This relation can be used to describe the drug dissolu- tion of several types of modified pharmaceutical dosage

release forms, particularly with low soluble drugs.[12]

## 2.4 First Order Kinetics

The application of this model was first proposed by Gibaldi and Feldman,<sup>39</sup> and later by Wagner.<sup>40</sup> The dissolution rate of the drug is described by the Noyes-Whitney equation as shown below:

$$dC$$

$$dt = K(C_s - C) \quad (3)$$

Where  $C$  is the concentration of solid in bulk dissolution medium,  $C_s$  is the concentration of solid in diffusion layer surrounding solid,  $K$  is a first order constant and it is associated with surface area of the solid drug, diffusion coefficient and diffusion layer thickness. Since the dissolution mechanism of drug is very complex, various empirical equations are proposed to describe this process. For example, the popular Weibull equation expressed the fraction of drug,  $m$  at time  $t$ , in the simple exponential form: Where  $k_B$  is the Boltzmann constant,[13]  $T$  is the temperature,  $\mu$  is the viscosity of fluid medium and  $r$  is the NP radius. The biorecognition of the targeted drug delivery site is similar to a key lock mechanism which is in reality a complex[14] biochemical reaction. To depict the effect of adsorption of nanoparticles on a functionalized surface, Langmuir reaction model is employed.<sup>42</sup> The ligand-receptor binding process is a weak reversible process, which leads to continuous attachment and detachment of nanoparticles.<sup>43</sup> The material balance for the active surface including surface diffusion and the reaction rate expression for the formation of the adsorbed species  $c_s$  is defined by:[15]

$$c$$

$$t + \nabla \cdot (-D_s \nabla c_s) = k_a c_w - k_d c_s \quad (8)$$

Where  $D_s$  is the surface diffusivity ( $m^2/s$ ),  $c_w$  is the bulk concentration of the species at solid wall (unit  $mol/m^3$ ),  $\delta$  is the surface concentration on the active site ( $mole/m^2$ )

Table I. Mathematical models used to describe drug dissolution curves.

Zero order First order Hixson-crowell

Higuchi

Baker-lonsdale

$$\ln Q_t = \ln Q_0 + K_1 t$$

$$1 - 3 \quad 1 - 3$$

$$3/2 [1 - (1 - Q/Q_\infty)^2]^{1/3} - 1 = K_1 t \quad Q/Q_\infty = K_1 t$$

$$m = 1 - \exp(-a)$$

Korsmeyer-peppas Quadratic Logistic

$$Q/t \quad Q$$

$$Q_t = 100(K=1$$

$\infty$

$K_{tn}$

$\infty$

$k$

$t_2 + K_{t1}$

Where  $a$  is time related constants,  $T_i$  stands for the duration till the dissolution begins, while  $b$  is a parameter that describes the curve. as well as the adsorbed species'  $c_s$  surface concentration (mol/m<sup>2</sup>). Keep in mind that the units of  $c_s$  and  $c$  reflect their differences. The rates of adhesion and detachment are represented by  $k_a$  (m<sup>3</sup>/mol/s) and  $k_d$  (s<sup>-1</sup>), respectively. Still, the amount of adsorbed species multiplied by the overall concentration of active sites equals the concentration of active sites. The reaction rate equation is therefore given by:

the nanoparticle transportation diffusion and biochemical reaction dynamics in a channel. In this model, the con-vection diffusion in 2D fluid domain is coupled with the adhesion reaction occurring on the reaction surface (dis-ease site). When a portion of the blood vessel is injured, significant P-selectin is expressed on damaged endothelial cells, which can be targeted by nanoparticles coated with GPIb ligand. In this model, the convection-diffusion pro-cess of nanoparticle in 2D fluid domain is coupled with the adhesion reaction occurring only on the reaction sur-face which mimics the target site for drug delivery. The physical parameters used to create this model are listed in Table II. To initiate adhesion, nanoparticles must stay close to the vessel wall, inside the so called depletion layer also known as a near-wall layer where adhesion process take place. The thickness of the depletion layer is largely influ-enced by the flow rate, evident from the simulation results shown in Figure 3. When drug particles bind with the receptors coated surface, drug concentration drops near the surface, effectively forms a “depletion layer” near the wall.

Table II. Physical parameters used in nanoparticle binding in a channel.

Symbol	Value	Definition
$c_0$	1000 [mol/m <sup>3</sup> ]	Initial concentration
$k_a$	10 <sup>-6</sup> [m <sup>3</sup> /(mol*s)]	Adhesion rate constant
$k_d$	10 <sup>-3</sup> -10 <sup>-6</sup> [1/s]	Detachment rate constant
80	1000 [mol/m <sup>2</sup> ]	Active site concentration
$D_s$	10 <sup>-11</sup> [m <sup>2</sup> /s]	Surface diffusivity
$D$	10 <sup>-9</sup> [m <sup>2</sup> /s]	Particle diffusivity in the fluid
$k_B$	1.38 × 10 <sup>-23</sup> [m <sup>2</sup> kg s <sup>-2</sup> K <sup>-1</sup> ]	Boltzmann constant
$T$	300 [K]	Absolute temperature
$U$	0–25 [dyne/cm <sup>2</sup> ]	Maximum shear rate
$h$	10 <sup>-10</sup> [m]	Equilibrium bond length

Fig. 3. Nanoparticle binding in a channel at a flow rate of 0.1 and 1 mm/s respectively. As the flow rate increases the depletion layer thickness decreases due to greater nanoparticle flux and shorter retention time of the nanoparticles.

2.5.Nanoparticle Deposition and Distribution in aBlood Vessel Network

Another example application of continuum model is to determine nanoparticle deposition[16] and distribution in a complex vascular geometry. Figure 4 shows the drug delivery process in an idealized vascular network with three generations. The physical parameters used to create this model in listed in Table III. Drug loaded nanoparticles of a given concentration areinjected at the top inlet and are transported through the vascular network along with fluid flow. The left branchof the network is assumed to be a receptor coated target surface that can form bonds with ligands on drug loadedFig. 4. (A) Drug injected at the top inlet of an idealized vascular network with three generations; (B) Receptors coated vessel section in the left branch of vascular network.

Table simulation.	III.Physical parameters	used for blood vessel network
Symbol	Value	Definition
$c_0$	1000 [mol/m <sup>3</sup> ]	Initial concentration
$k_a$	10 <sup>-6</sup> [m <sup>3</sup> /(mol*s)]	Adhesion rate constant
$k_d$	10 <sup>-9</sup> [ 1/s]	Detachment rate constant
80	1000 [mol/m <sup>2</sup> ]	Active site concentration
$D_s$	10 <sup>-11</sup> [m <sup>2</sup> /s]	Surface diffusivity
$D$	10 <sup>-6</sup> [m <sup>2</sup> /s]	Particle diffusivity in the fluid
$V$	1 [mm/s]	Maximum velocity
$\rho$	1063 [kg/m <sup>3</sup> ]	Blood density
$\eta$	0.003 [Pa.s]	Blood dynamics viscosity

The density of deposited drug particles on the wall surface is plotted in Figure 5, which indicates that most drug particles are deposited at the entrance of the target region, while the rest of the target region has low density of deposited drug particles. There[16]

to reveal that particle shape may have a profound effect on their biological properties. For example, cylindrically shaped filomicelles can effectively evade the non-specificuptake by the reticuloendothelial systems and persisted in the circulation up to one week after intravenous injection.From drug delivery stand point of view, non-spherical particles will allow larger payload delivery than the spherical counterpart with same binding probability. Recently, Mitragotri and coworkers have shown that the local shape are no particles deposited in the healthy branchDhedliuveetroedanby Ionfgtehnetpaartot ic:le at the point where a macrophage is attached, assumption of zero non-specific adhesion at that particGuulaerst Unsoetr the overall shape, dictated whether the cell began location. Such non-uniform distribution pattern inIdPica:te7s6.98i.n2t.e4rn1alization.51 These results indicate the importance of possible impaired delivery dosage within theStuarng,e2t r9egAiopnr, 201c2on0tr1o:l3li9ng:0p9article shape for nanomedicine application. which is important for delivery efficacy prediction anddosage planning.

3. Particulate Approach: Rationaldesign Of Nanoparticles

3.1. Introduction to Nanoparticle Design

Most of the nanoparticles employed in the experimental studies are spherical in shape. Extensive studies have been. Theoretical studies of nanoparticle deposition are typically focused on simple spherical or oblate shape.<sup>52–54</sup> Ideally, there should be a tool that can handle variety of shapes and sizes of nanoparticles, which enables endless possibilities of finding most suitable design of the nanoparticle for a given application. Decuzzi and Ferrari.<sup>52–54</sup> have studied the margination of nanoparticles in blood stream, where nanoparticles diffusion in Newtonian fluid has been analyzed. The same authors have also examined the adhesion probability of nanoparticles under an equilibrium<sup>[17]</sup>

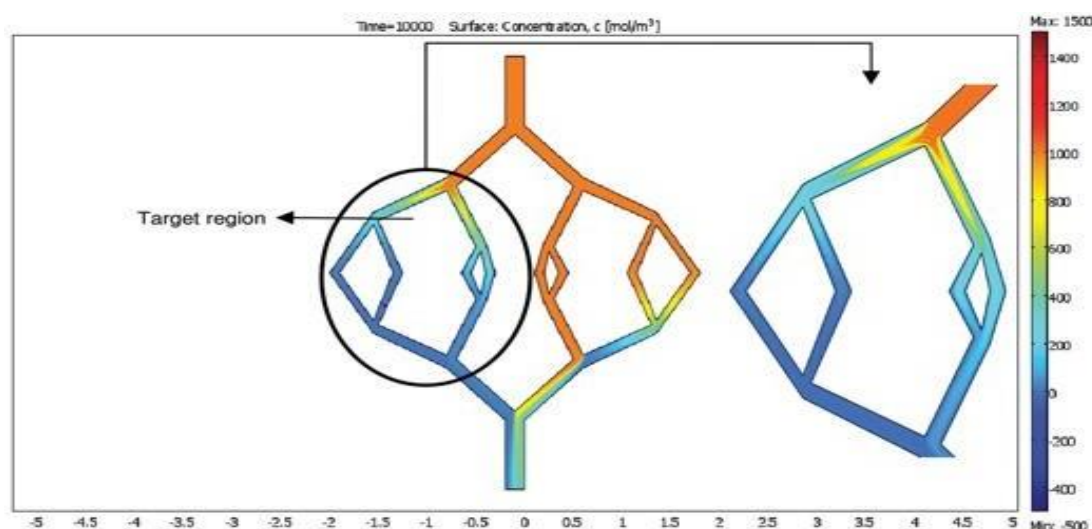


Fig. 1. Drug concentration as it flows from parent vessel through the vascular network with the receptor coated target region marked by the black circle. Red color indicates highest concentration, while blue color indicates lowest concentration.

nanoparticles' sizes, shapes, and surfaces, as well as their transport phenomena and the binding combinations that each parameter may achieve (Geuffie-st The likelihood of nanorods and nanospheres undergoing shear-cient focused delivery is minimised. An overwhelming number of IP addresses (7o6f.98.fl2o.w41) have been research focused on characterising nanoSpaurnti,cl2e9pAhypsir- 201o2f 0n1an:3or9o:d0s9, where their tumbling motion and greater con- real estate. Using dissipative particle dynamics, [18]Djohari and Dormidontova<sup>57</sup> investigated the kinetics of spherical nanoparticles targeting the surface of cells. The adsorption geometry configuration. Mody et al.<sup>55,56</sup> studied platelet motion near vessel wall surface under shear flow and concluded that hydrodynamic force influences platelet adhesion to the wall surface. The same authors<sup>55,56</sup> also investigated the influence of Brownian motion on platelet movement and found that Brownian motion does not influence platelet- shaped cells at physiological shear rates. However, size( 2  $\mu\text{m}$ ) and shape (oblate) of the platelet is not compa- rable to that of nanoparticles and the behavior observed for platelet might not be applicable for nanoparticles<sup>[19]</sup>.

### 3.2. Influence of Nanoparticles Size and Shape on Targeted Delivery

The targeted drug delivery process in general can be considered as a seamless combination of three stages: transport through the vessel network; adhesion process; and cellular update.



Each stage is effectively governed nanoparticle was found to become ellipsoidal with increasing binding energy. Janus-like nanoparticles[20] with ligands coated on one side of the nanoparticle was observed to bind faster than that with uniformly coated ligands. Genget al.58 revealed the potential of non- spherical shaped carrier for drug delivery application. Figure 6 shows the results of their experimental study on the circulation time of filomicelles of different lengths in a mice model. Further, the same group performed in vivo study to investigate the shape effect and discovered that non-spherical shape carrier has 10 times longer circulation time compared to its spherical counterpart. Muro et al.59 studied controlled endothelial targeting and intracellular delivery by modulating size and shape of the drug carrier. Their study found that carrier geometry influences endothelial targeting efficiency. The non-spherical carrier had longer circulation time and higher targeting specificity than regular spherical carrier. Shah and Liu tact area.46,60,61 Winter et al.62 and Liu et al.63,64 have performed numerical simulations of dielectrophoresis of non-spherical particles. Theoretical models to determine

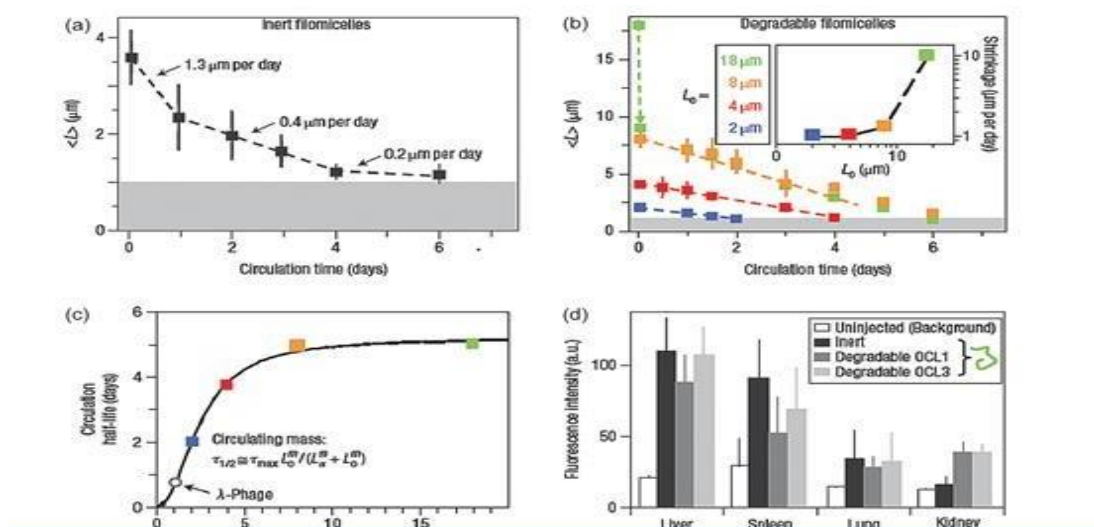


Fig. 6. Kinetics of filomicelle length reduction in vivo. (a) Inert filomicelles shorten, with the rate of shortening decreasing as they shorten. The grey region represents the optical limit of  $L$  measurements; (b) Degradable filomicelles (OCL3) shorten at a rate that depends on initial length. The inset plots the length dependent shrinkage rate; (c) Filomicelles show a saturable increase in half-life of circulating mass, fitting a cooperative clearance model with  $\tau_{max} = 5.2$  days,  $m = 2.1$  and  $L_0 = 2.5$  μm; (d) Distribution of inert and degradable filomicelles in clearance organs for  $L_0 = 4$  or 8 μm after four days in the circulation of rats. All error bars show the standard deviation for three or more animals. Reprinted with permission from [58] Y. Geng, et al., Shape effects of filaments versus spherical particles in flow and drug delivery. *Nat. Nanotechnol.* 2, 249 (2007). © 2007, Macmillan Publishers Ltd: Nature. adhesion probability of different shaped nanoparticles is discussed in the next section.

### 3.3. Theoretical Model of Nanoparticle Adhesion Probability

The cell targeting process of nanorods and nanodisks under flow conditions is described using a computational model that is based on the work of Decuzzi and Ferrari52,65. The *Nanotechnology Perceptions* Vol. 20 No. S14 (2024)



probabilistic kinetic formulation of McQuarrie<sup>66</sup> and Decuzzi<sup>67</sup> is used to characterise the adhesion probability ( $P_a$ ) for spherical<sup>[21]</sup> particles of same volume. The disc-shaped nanoparticles outperform their spherical counterparts by a factor of 300 when it comes to cell targeting and by a factor of 40 when it comes to drug loading, thanks to their superior adhesion probability and huge volume to mass ratio. A rod-shaped particle with an aspect ratio of 5 has an adhesion probability that is about twenty times greater than that of a spherical particle. Across all volume ranges, oblate-shaped nanoparticles have an adhesion probability that is almost ten times greater than that of spherical particles. The dynamic process of nanoparticle transport and administration<sup>[22]</sup> is not shown by this theoretical model, which is predicated on the adhesion probability for a particle to attach to a receptor coated surface. Interconnected models that combine This model, which can be used to nanoparticles of different shapes, is still in its early stages of development. It takes into account the receptor density on the substrate surface ( $m_r$ ), the ligand density on the particle surface ( $m_l$ ), the contact area of the particle ( $A_c$ ), and the force acting per unit margin ( $f$ ).

This process analysis for a randomly formed The thermal energy of the ligand-receptor pair, denoted as  $kBT$ , is determined by a multiscale model. This model is essential for determining the characteristic length of the ligand-receptor bond and for gaining biological insights into the transportation and adhesion kinetics of the ligand-receptor pair at zero IPLO: a7d.6.98s.i2o.n41. The following will first present Examining the theory and model of normalised adhesion kinetics for oblate-, Sroudn-, a2n9d dAispcr- 201th2e01na:3no9p:0ar9ticles Figure 7 shows the relationship between particle volume and the form of nanoparticles subjected to a wall shear stress of 1 (Pa). It is decided that the aspect ratio of the rod (length over diameter) and the disc (diameter over height) would be 5. Figure 7 shows that when the volume of a spherical particle grows, the adhesion probability rises initially because there is more surface area available for bond formation, but subsequently falls as the volume diminishes. A lower likelihood of adhesion exists<sup>[23]</sup> for bigger particles because the dislodging force acting on such particles is greater than the binding forces, washing them away. The non-spherical particles' critical volume is quite big and moves to the right side of the plot (out of the plot range) as a result of the shape effect. The adhesion probabilities of the oblate, rod, and disc particles are noticeably greater than those of the

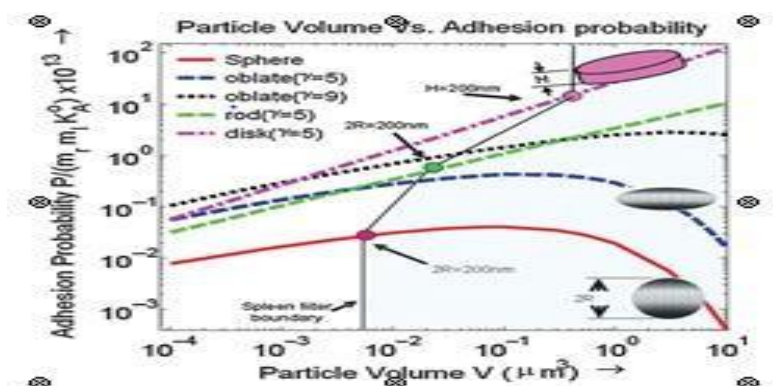


Fig. 7. Adhesion probabilities of nanoparticles of various shapes as a function of particle volume,  $\gamma$  is the aspect ratio. method. Then, adhesion process and trajectories for

nanoparticles of different shapes and ligand densities are presented. Next, the binding probability of nanoparticles is determined for a range of channel sizes.

### 3.4. Particulate Model of Nanoparticle Delivery in a Vascular Environment

Nanoparticles are usually introduced into the vascular circulation stream through intravenous injection.<sup>68–70</sup> The targeted delivery efficiency is directly related to the nanoparticle selectivity and ability to bind at the targeted site. Though highly selective nanoparticles have reduced binding probability in non-target regions, the majority of nanoparticles are still lost in the vascular network due to non-specific adhesion. It is thus important to predict vanished concentration of nanoparticles in the upstream and nanoparticle concentration when it reaches the targeted region. The focus of a particulate model is to explore an optimum design of nanoparticle to achieve high binding probability in the diseased region and high overall delivery efficiency under given vascular environment.

#### 3.4.1. Nanoparticle Adhesion Kinetics

To achieve targeted drug delivery, nanoparticles are usually coated with ligands that bind specifically to a particular type of receptors expressed on the diseased vessel cell surface.<sup>71</sup> Once nanoparticles marginate to vascular surface, the ligand coated nanoparticles interact with the specific receptors expressed at target surface. Such interaction results in a bond formation between nanoparticle and vascular surface. The adhesive strength of bond is mediated by the specific binding of ligand-receptor. Other factors such as steric interactions, electrostatic, van der Waals (vdW) or hydrodynamic forces also influence interactions between nanoparticle and vessel surface. However, the vdW force is usually several orders of magnitude smaller compared to specific adhesive force, whilst the effect of steric interaction and electrostatic is limited to very short distance (less than nanometer scale).<sup>53</sup> Thus, these factors are neglected for this model. The ligand-receptor binding process is integrated with Brownian dynamics and this combined model is embedded into the Immersed Finite Element (IFEM) platform.<sup>72–75</sup> IFEM can be used for fully coupled fluid-structure interaction problems, i.e., solving particle motion in a fluid while capturing the influence of particle on fluid flow. However, due to Brownian motion, it is computationally expensive to calculate the change of fluid flow caused by particle motion at every time step.  $k_0$  are the reverse and forward reaction rates at zero load of ligand-receptor pair, respectively;  $L$  is the difference between bond length  $y$  and equilibrium length  $h$ . During dynamic interaction process, the bond length of a ligand-receptor pair may vary based on particle location. The ligand-receptor bonds are modeled as springs with spring constant  $\sigma$  and equilibrium length  $h$ , thus the bond forces are described as a function of bond length  $y$ .<sup>[25]</sup> Then, the ligand-receptor interaction forces can be summed on finite element surface through integration over the nanoparticle surface. Equations of bond forces  $f_L$  and integrated adhesion forces  $\sigma_s$  on particle surface  $\Gamma$  are given as:

$$f_L = \sigma(y - h) \quad (15)$$

∫

$$\sigma \mathbf{S} \cdot \mathbf{n} = N b f_L(X_c) d\Gamma \quad (16) \text{ process.}$$

When a particle approaches the vascular wall, ligands on the particle surface form bonds with receptors on the

vascular wall, as demonstrated in Figure 8. An adhesion kinetic equation is used to calculate the bond density  $N_b$ :

$N_b$

$$\dot{N}_b = k_f(N_l - N_b)(N_r - N_b) - k_r N_b \quad (12)$$

Where  $N_l$  and  $N_r$  are the ligand and receptor densities;  $k_r$  and  $k_f$  are the reverse and forward reaction rates, respectively. This interaction model represents a conservation equation of the different species (ligands, receptors, and bonds). The  $k_r$  and  $k_f$  are function of bond length:

$$k = k_0 \exp(-(k - k_0)L^2/2B_z) \quad (13) \quad k_f = k_0 \exp(-k_{ts}L^2/2B_z) \quad (14)$$

Where  $k_s$  is the bond elastic constant;  $k_{ts}$  is the bond elastic constant at transient state;  $B_z$  is thermal energy;  $k_0$  and  $k_{ts}$  are important and are integrated into the IFEM formulation by adding a Brownian force term, which is described in the next section.

### 3.4.2. Brownian Dynamics at Nanoscale

Fundamental theories of Brownian dynamics have indicated that random collisions from surrounding liquid molecules impacts motion of an immersed small particle.<sup>79–81</sup> The influence of Brownian motion on behavior of nanoparticles in microfluidic channel and platelets and blood cells in blood flow has been studied extensively.<sup>82–85</sup> Patankar et al.<sup>86</sup> have proposed an algorithm for direct numerical simulation of Brownian motion by adding random disturbance in fluid. At microscale, the drag force acting on particles such as blood cells is significantly large ( $>50$  pN for particle size  $>1 \mu m$ ), thus Brownian motion is neglectable.<sup>82</sup> At nanoscale, Brownian force becomes a dominant force to drive nanoparticle near vascular wall surface, while the drag force acting on a nanoparticle is relatively small. Shah and Liu et al.<sup>60</sup> developed novel hybrid model to study Brownian dynamics at nanoscale and governing equations are described as following.<sup>[28]</sup>

The random forces  $R(t)$  and torque  $T(t)$  acting on a nanoparticle is responsible for Brownian motion and rotation and satisfy the fluctuation-dissipation theorem:<sup>87</sup>

$$\langle R_i(t) \rangle = 0, \quad \langle T_i(t) \rangle = 0 \quad (17)$$

$$\langle R_i(t) R_j(t_r) \rangle = 2k_B T \beta_{ij} \delta(t - t_r),$$

Where  $\beta$  is the unit-second order tensor,  $\delta_{ij}$  is the Kronecker delta,  $\delta(t - t_r)$  is the Dirac delta function,  $k_B T$  is thermal energy of system,  $\beta_t$  and  $\beta_r$  are the translational and rotational friction coefficient of nanoparticle, The friction coefficient of a rod-shaped particle for an arbitrary orientation is given by Ref. [92]:

$$\beta_t = 3\eta \mu_{eqv} \times (\cos^2 \theta + \frac{1}{2} \sin^2 \theta) \quad (19) \text{ respectively.}$$

$$\beta_r = \eta \mu_{eqv} \quad (20)$$

parameters, such as fluid viscosity, size and shape of nanoparticle.  $\mu$  is the fluid viscosity,  $\mu_{eqv}$  is the diameter of nanoparticle. The friction coefficient for spherical nanoparticle. The friction coefficient for spherical nanoparticle. The friction coefficient for spherical nanoparticle. There is no empirical formula available for determining the friction coefficient of particles with complex shapes. In literature, there are empirical formulas for friction coefficient Stokes correction factors for a spheroid particle moving parallel and perpendicular to

the flow, respectively. These correction factors are expressed as Ref. [92]: coefficients for 9p2 articles, but limited to simple shapes and orientations such as oblate or rod-shaped particles. In a recent work by Loth, a new empirical formula is proposed to compute friction coefficient for a non-spherical particle. Friction coefficient of rod shaped particles in this work is derived based on Loth and extended with an angle factor to incorporate arbitrary orientations. When a particle travels along the fluid flow, the relative velocity of the particle can be divided into components in two directions: Where  $\zeta$  is the aspect ratio of the spheroid particle. The velocity of a particle moving under a deterministic force in a fluid with velocity  $V_f$  is given by:

parallel to flow and perpendicular to flow, as shown in Figure 9.

$V_s =$

$F_{det} + V$

$\beta t \quad f$

$$(1 - e^{-(\beta t / m)t}) \quad (23)$$

Where  $V_s$  represents the velocity of the solid and  $V_f$  represents the velocity of the fluid, and  $F_{det}$  is the total deterministic force acting on the nanoparticle (including Brownian force, adhesion force, etc.). Equation (24), at a time step (usually 1  $\mu s$ ), states that the drag force from the fluid balances the deterministic force acting on a particle. Since the mass of a nanoparticle is so little, the inertia effect may be disregarded, which makes sense. The nanoparticle's translational location is then updated using this terminal velocity. Similarly, one may determine a nanoparticle's angular velocity by Where  $c_f$  is the angular velocity due to fluid flow. Combining the translational and angular velocities, particle nodal positions are updated based on its distance from the particle center as:

$$v_i = V_s + c_s \times r_i \quad (26)$$

The fluid flow in our simulation is assumed to be an incompressible viscous fluid governed by the Navier-Stokes equations:

load capacity. The simulations are carried over a channel of 5  $\mu m$  long and 2  $\mu m$  high. In the simulation, a spherical particle and a rod-shaped particle are initially positioned with their centers 600 nm above a receptor-coated surface, as shown in Figure 10.

A velocity is applied at the top of channel to generate a shear rate of 8.0  $s^{-1}$ . Nanoparticles are allowed to move freely through the channel under the influence of shear flow and Brownian forces. For a typical simulation demonstrated in Figure 10, the spherical particle fails to make

$$\nabla \cdot v_f = 0 \quad (28)$$

It should be noticed that  $v_f$  is the fluid velocity in the fluid main, while  $V_f$  is the fluid velocity interpolated onto the solid domain. The Navier-Stokes equations are solved

Simulation Results of Nanoparticle Targeted Delivery Process

Mathematical modeling of targeted drug delivery system provides quantitative description of the drug transportation in biological systems. Therefore, it can be utilized to evaluate

efficiency of drug delivery and to estimate dose response.

### 3.4.3. Effect of Nanoparticle Shape on Adhesion Kinetics

What follows is a discussion of how the shape of nanoparticles affects the rate of adhesion. The near-wall behaviour of spherical and non-spherical particles has been assessed in two independent sets of simulation simulations. Nanoparticle Deposition Process Comparison. Two nanoparticles, one spherical and one non-spherical, with the same volume, are considered in this work to examine the effect of nanoparticle form on adhesion kinetics. This rod-shaped particle has an aspect ratio of 5 and a length of 1000 nm. A spherical particle has a diameter of 380 nanometers. To learn whether nanorods or nanospheres adhere well to the wall surface for a specific drug-owing adhesion force, which guarantees strong adhesion and, eventually, equilibrium with complete contact, it is helpful to compare their volumes constantly. The simulation findings show that nanorods and nanospheres often exhibit distinct dynamic adhesion mechanisms, as seen by their usual trajectories. Subsequent sections will provide a quantitative account of the adhesion process.

The very existence of such near-wall particle tumbling motion is an issue that may emerge at this stage. It has been shown in literature that non-spherical particles may tumble close to the surface of a wall.<sup>56,95, 96</sup> It has been discovered that nanorod rotation is enhanced when shear flow and Brownian rotation are coupled.<sup>97.</sup> 48 percent Analysing Nanorod and Nanosphere Trajectories. The tumbling motion of nanorods makes them more likely to come into contact with the wall surface than their spherical counterparts. By comparing the trajectories of spherical and non-spherical nanoparticles subjected to the same flow condition, this idea may be tested. Both instances make use of a shear rate of  $8.0 \text{ s}^{-1}$ . The  $15 \text{ }\mu\text{m}$  in length and  $5 \text{ }\mu\text{m}$  in height channel is used for the simulations. As demonstrated in Figure 11(A), the oscillations of the nanoparticle-wall distance are shown by recording the lowest distance between the nanoparticle surface and the wall surface over time. As the nanoparticle travels through the channel, its trajectory follows this pattern. At the beginning of a sequence of simulation runs, a nanorod and a nanosphere are positioned  $650 \text{ nm}$  above the surface of the wall. Figure 11(B) shows the nanorod and nanosphere trajectories from 20 separate simulations. A nanorod's trajectories exhibit bigger variations as a consequence of its tumbling motion, as shown by the simulation results.

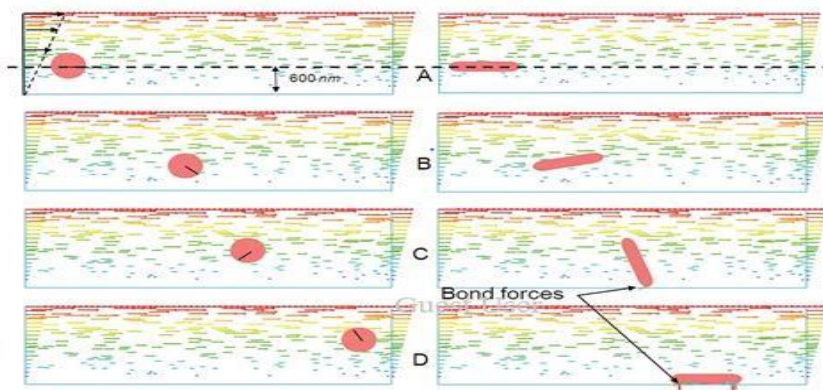


Fig. 10. Shape dependent particle adhesion kinetics. The left cIoPlum: n7s6ho.9w8s



a spherical particle washed away without contact with surface; the right column shows a nanorod tumbles and gets deposited. SAu, nB, 2C, 9DAAprera2t t0im1e2s t0=1:03s9, :00.295 s, 0.5 s, and 0.75 s, respectively. The line labeled on the spherical particle indicates its rotation. The vectors in fluid domain indicate flow field and arrows indicate magnitude and direction of bonding forces.

thus it has more contact/adhesion events compared to that of nanosphere, as shown in Figure 11(C). Moreover, in a fixed number of trials, ten nanorods are deposited while only three nanospheres are deposited. Probability of spherical particle to contact with wall surface solely depends on Brownian diffusion; while in case of non-spherical particle, probability of contact is enhanced by tumbling motion. Thus, this result indicates that nanorod has higher contact probability than the nanosphere for given physiological flow condition.

#### 3.4.4. Nanoparticle Binding Probability

A thorough approach to modelling the whole adhesion and transportation dynamics of nanoparticles with any form has been devised in the preceding sections' simulation technique. Deriving a binding probability for nanoparticles under different configurations is computationally cost-effective and more convenient for modelling the adhesion process of huge numbers of nanoparticles. If a nanoparticle is close enough to the vascular wall, it has a particular binding probability and will likely bond to the wall. Out of all the nanoparticles in the fluid channel, how many will bond to the wall surface? This is determined by the binding probability. In order to determine the optimal medication concentration for a certain application, this parameter is crucial. Keep in mind that this section only deals with nanoparticles. Researchers have shown that blood cells may affect how quickly nanoparticles disperse. Having said that Understanding how particle form affects binding property is the main objective of this section. However, further research and development will be necessary to encompass multi-scale models that can handle nanoparticles and blood cells in the future. The creation of bonds may only begin when nanoparticles remain in close proximity to the wall surface, inside a cell free layer (CFL) or depletion layer,<sup>99</sup> as seen in Figure 12. Near the vessel wall, pure plasma flows at a slower rate than the red blood cells, which are moving at a relatively higher velocity in the vessel's centre. It is reasonable to limit consideration of deposition to nanoparticles due to the presence of CFL. For vessels with a diameter more than 20  $\mu\text{m}$ , the cell free layer thickness is seen to range from 2 to 5  $\mu\text{m}$ , regardless of the size of the vessel.<sup>100–102</sup> [27][28].

This indicates that different depletion layer or CFL thicknesses should have their binding probabilities investigated. In this section, we examine how the nanoparticle binding probability is affected by two parameters: shear rate and depletion layer thickness. Every example has the same set of parameters since we want to analyse the influence of the ones we've already discussed consistently. For instance, it is generally believed that the ligand density is high enough to ensure that nanoparticles adhere firmly (the adhesion force usually ranges from 1 pN to 100 pN, whereas the dislodging forces are restricted to around 0.01 pN). Additionally, new evidence suggests that nanoparticles are very resistant to hydrodynamic forces once they attach to a receptor-coated surface.<sup>103</sup> because of the strong adhesive force that dominates all other forces work would be crucial tool for engineering shape and size of these nanocarriers. As a result, there have been a significant growth in the number of papers



on modeling nanoparticle targeted delivery published lately 46,60,61,105,106 as shown in

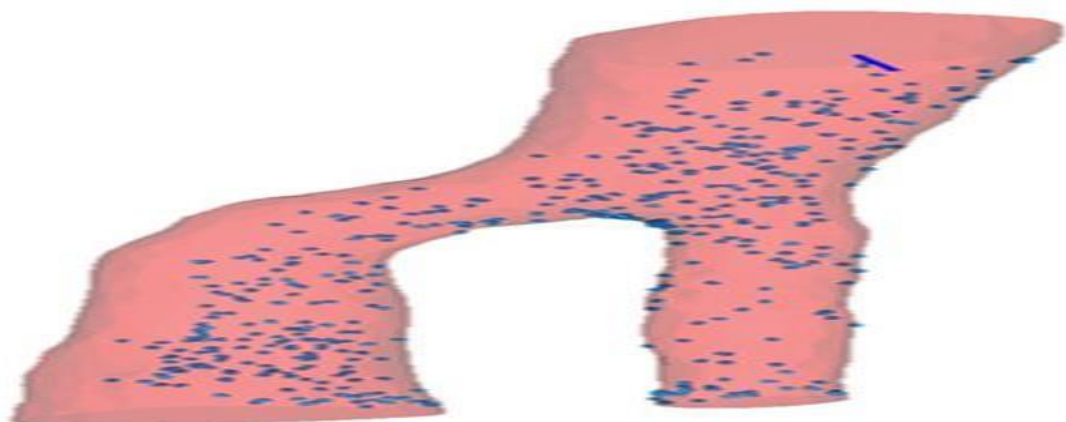


Figure 15: there have been a significant growth in the number of papers on modeling nanoparticle targeted delivery

#### 4. Conclusion

Multi-scale modeling of targeted drug delivery system provides quantitative description and in-depth analysis of the drug transportation and delivery process in dynamic biological system. Such detailed results are very useful to determine delivery efficiency of particular nanocarrier for a given vascular condition and indeed to estimate dose quantity and toxicity. An accurate computational model needs to represent the actual physiological condition of drug delivery. Most current studies focus on modeling nanoparticle transport and binding under idealized vascular environment such as simple straight and branched channels. To mimic the real vascular environment, the vascular geometry could be reconstructed from CT/MRI scanned images. The simulated nanoparticle deposition in a branch vessel reconstructed from MRI scanned images is shown in Figure 16. Such virtual tool can be used to predict nanocarrier bio-distribution and the delivery efficiency under a given patient vascular geometry and hemodynamic conditions, and help design nanoparticles for maximum targeting efficiency and minimum drug dosage. Using intelligent biomaterials in microfabricated and nanoscale devices to transport pharmaceuticals,

#### References

1. C. Roney, P. Kulkarni, V. Arora, P. Antich, F. Bonte, A. M. Wu, N. N. Mallikarjuna, S. Manohar, H. F. Liang, A. R. Kulkarni, H. W. Sung, M. Sairam, and T. M. Aminabhavi, "Targeted nanoparticles for drug delivery through the blood-brain barrier for Alzheimer's disease," *Mrs. Bulletin*, vol. 31, no. 888, pp. 193, 2006.
2. P. Shah, "Use of nanotechnology in medication administration," *Releasing Controlled Substances*, vol. 108, pp. 193, 2005.
3. G. B. Sukhorukov and H. Mohwald, "Multifunctional cargo systems for biotechnology," *Trends in Biotechnology*, vol. 19, pp. 25–93, 2007.
4. W. T. Al-Jamal and K. Kostarelos, "Liposomes: Transitioning from a nanoparticle platform for *Nanotechnology Perceptions* Vol. 20 No. S14 (2024)

- therapeutic nanomedicine to a drug delivery system with a clinical track record," *Chemical Research Reports*, vol. 44, pp. 1094, 2011.
  5. G. Sharma, S. Anabousi, C. Ehrhardt, and M. N. Ravi Kumar, "Liposomes as targeted drug delivery systems in the treatment of breast cancer," *Pharmaceutical Targets*, vol. 14, pp. 301, 2006.
  6. R. P. Choudhury, V. Fuster, and Z. A. Fayad, "Imaging of atherothrombosis: molecular, cellular, and functional findings," *Review of Drug Discovery in Nature*, vol. 3, pp. 913, 2004.
  7. A. Eisenberg, D. Maysinger, J. Lovric, and R. Savic, "How micelles and quantum dots perish within cells," *Eur. J. Pharm. Biopharm.*, vol. 65, pp. 270, 2007.
  8. D. Sutton, N. Nasongkla, E. Blanco, and J. Gao, "Functionalized micellar systems for cancer targeted drug delivery," *Pharmaceutical Research*, vol. 24, pp. 1029, 2007.
  9. V. P. Torchilin, "Targeted polymeric micelles for delivery of poorly soluble medicines," *Journal of Cellular and Molecular Biology*, vol. 61, no. 25, pp. 2549, 2004.
  10. S. Nie, J. W. Simons, F. F. Marshall, L. Yang, J. A. Petros, and X. Gao, "Molecular and cellular imaging using quantum dots in living organisms," *Trends in Biotechnology*, vol. 16, pp. 63, 2005.
  11. A. M. Smith, G. Ruan, M. N. Rhyner, and S. Nie, "Engineered luminous quantum dots for in vivo molecular and cellular imaging," *Ann. Biomed. Eng.*, vol. 34, no. 3, pp. 345, 2006.
  12. S. Koenig and V. Chechik, "Nanoparticles of shell-cross-linked gold," *Journal of Langmuir*, vol. 22, pp. 5168, 2006.
  13. X. Lou, C. Wang, and L. He, "Core-shell Au nanoparticle formation with DNA-polymer hybrid coatings using aqueous ATRP," *Biomacromolecules*, vol. 8, no. 1385, 2007.
  14. Y. Cheng, Y. Gao, T. Rao, Y. Li, and T. Xu, "Prodrugs based on dendrimers: Design, synthesis, screening, and biological assessment," *High Throughput Screen*, vol. 10, pp. 336, 2007.
  15. R. Duncan and L. Izzo, "Toxicology and biocompatibility of dendrimers," *Journal of Advanced Drug Delivery*, vol. 57, pp. 2215, 2005.
  16. M. Najlah and A. D'Emanuele, "Dendrimer nanotechnologies for cellular barrier crossing," *Current Pharmaceutical Practice*, vol. 6, pp. 522, 2006.
  17. C. G. Galbraith and M. P. Sheetz, "Pressures exerted on adhesive contacts influence the activity of cells," *Cell Biology: A Current Opinion*, vol. 10, pp. 566, 1998.
  18. W. R. Sanhai, J. H. Sakamoto, R. Canady, and M. Ferrari, "Seven obstacles in nanomedicine," *Nanotechnology*, vol. 3, pp. 242, 2008.
  19. R. J. Shipley and S. J. Chapman, "Multiscale modelling of fluid and medication transport in vascular tumours," *Biometrics*, vol. 72, pp. 1464, 2010.
  20. S. Modok, R. Scott, R. A. Alderden, M. D. Hall, H. R. Mellor, S. Bohic, T. Roose, T. W. Hambley, and R. Callaghan, "Approximating the impact of diffusion on reversible processes at the cell surface: Ligand- receptor kinetics," *Biophysical Journal*, vol. 68, pp. 1222, 1995.
  21. B. D. Chithrani, A. A. Ghazani, and W. C. W. Chan, "Investigating the relationship between the size and form of gold nanoparticles and their absorption into cells of mammals," *Nano Letters*, vol. 6, pp. 652, 2006.
  22. C. Allen, H. Lee, B. Hoang, and R. M. Reilly, "Polymeric nanoparticle intratumoral and subcellular distribution as a function of particle size and molecular targeting," *Molecular Pharmaceutics*, vol. 7, pp. 1195, 2010.
  23. D. A. Hammer and J. B. Haun, "The measurement of nanoparticle adherence induced by certain molecular interactions," *Langmuir*, vol. 24, pp. 8821, 2008.
  24. N. Nishiyama, "Nanocarriers form for extended lifespan," *Nature Nanotechnology*, vol. 2, pp. 1-2, 2007.
- Nanotechnology Perceptions* Vol. 20 No. S14 (2024)

- 203, 2007.
25. M. Ferrari, "Nanogeometry: More Than Just Drug Delivery," *Nature Nanotechnology*, vol. 3, pp. 131, 2008.
  26. S. Cai, D. Cheng, E. M. Lima, and D. E. Discher, "The benefits of worm-like filomicelles of PEO-PCL in paclitaxel administration," *Research in Pharmaceuticals*, vol. 24, pp. 2099, 2007.
  27. "Killing cells," *Journal of the National Academy of Sciences, USA*, vol. 103, pp. 4930, 2006.